

# A normal ocular motor system model that simulates the dual-mode fast phases of latent/manifest latent nystagmus

L. F. Dell'Osso<sup>1,2,3</sup>, J. B. Jacobs<sup>1,3</sup>

<sup>1</sup> Ocular Motor Neurophysiology Laboratory, Veterans Affairs Medical Center, Case Western Reserve University, 10701 East Boulevard, Cleveland, OH 44106, USA

<sup>2</sup> Department of Neurology, Case Western Reserve University and University Hospitals of Cleveland, Cleveland, Ohio, USA

<sup>3</sup> Department of Biomedical Engineering, Case Western Reserve University and University Hospitals of Cleveland, Cleveland, Ohio, USA

Received: 16 June 2000 / Accepted in revised form: 20 May 2001

**Abstract.** The fast phases of latent/manifest latent nystagmus (LMLN) may either cause the target image to fall within (foveating) or outside (defoveating) the foveal area. We previously verified that both types are generated by the same mechanism as voluntary saccades and propose a hypothetical, dual-mode mechanism (computer model) for LMLN that utilizes normal ocular-motor control functions. Fixation data recorded during the past 30 years from 97 subjects with LMLN using both infrared and magnetic search coil oculography were used as a basis for our simulations. The MATLAB/Simulink software was used to construct a robust, modular, ocular motor system model, capable of simulating LMLN. Fast-phase amplitude versus both peak velocity and duration of simulated saccades were equivalent to those of saccades in normal subjects. Based on our LMLN studies, we constructed a hypothetical model in which the slow-phase velocity acted to trigger the change between foveating and defoveating LMLN fast phases. Foveating fast phases were generated during lower slow-phase velocities whereas defoveating fast phases occurred during higher slow-phase velocities. The bidirectional model simulated Alexander's law behavior under all viewing and fixation conditions. Our ocular-motor model accurately simulates LMLN patient ocular motility data and provides a hypothetical explanation for the conditions that result in both foveating and defoveating fast phases. As is the case for normal physiological saccades, the position error determined the saccadic amplitudes for foveating fast phases. However, the final slow-phase velocity determined the amplitudes of defoveating fast phases. In addition, we suggest that individuals with LMLN use their fixation subsystem to further decrease the slow-phase velocity as the target image approaches the foveal center.

## 1 Introduction

Latent/manifest latent nystagmus (LMLN) is a specific type of infantile nystagmus that occurs subsequent to strabismus in some patients (Dell'Osso et al. 1979, 1983a). It may be confused with another type of infantile nystagmus, congenital nystagmus (CN), in patients with strabismus and a latent component to their CN (Dell'Osso 1985, 1994), or the nystagmus blockage syndrome (Dell'Osso et al. 1983b); the presence of a head turn further confounds the identification. Accurate eye-movement recordings can reliably differentiate LMLN from CN by identifying the respective waveforms and their variation with gaze and convergence angle. Unlike CN, whose amplitude grows as gaze is directed to either side of the null position, the amplitude of LMLN usually follows Alexander's law (i.e., it increases as the fixating eye moves into abduction and decreases in adduction (see Figs. 9 and 10 of Dell'Osso et al. 1979). The slow phases of LMLN may be either linear or have a decreasing velocity in the same patient. (Studies of the fast phases confirmed that they satisfied saccadic velocity- and duration–amplitude relationships – Erchul et al. 1996; Erchul and Dell'Osso 1997.) However, depending on the slow-phase velocity, LMLN fast phases could be programmed to cause the target image to fall either within (foveating) or outside (defoveating) the foveal area (Dell'Osso et al. 1995). Higher slow-phase velocities were found to precipitate defoveating fast phases (Erchul et al. 1998). Also, as presaccadic slow-phase velocities grew, fast-phase amplitude followed.

Several mechanisms have been proposed as the cause of LMLN. Confusion of egocentric direction secondary to strabismus may result in a constant-velocity drift of the eyes in the direction opposite to the fixating eye (Dell'Osso et al. 1979; Dell'Osso and Daroff 1981). Alternatively, it has been suggested that a nasotemporal asymmetry in the optokinetic system may cause the tonic drift of the eyes (Kommerell and Mehdron 1982). Finally, a proprioceptive imbalance has also been suggested as being responsible for the slow-phase genesis of LMLN (Ishikawa 1979). Each putative mechanism

---

Correspondence to: L. F. Dell'Osso  
 (Tel.: +1-216-4213224, Fax: +1-216-2313461  
 e-mail: lfd@po.cwru.edu)

results in a linear slow phase in the direction opposite to the fixating eye, although the proprioception hypothesis is limited to esotropia.

Our approach to modeling the ocular motor system is primarily based on function, dysfunction, and system-level responses. Although specific neuroanatomy and neurophysiology are incorporated into the model as much as possible (e.g., the retina, the extraocular muscle and globe plant, the ocular motor neurons, the common neural integrator in the vestibular and prepositus hypoglossi nuclei, and the pulse-generator burst cells of the pons), the absence of functional correlation for more centrally located sites does not preclude the incorporation of necessary hypothetical function into the model. Indeed, it is not clear that neurophysiological signals exist that parallel the functional signals of their models (Robinson 1994). Many neurological signals appear to be composites of several functional signals that cannot be decomposed into recognizable parts. With that caveat, it is interesting to note that recent work suggests that structures in the paramedian tract may contain many of the signals required by the functional block we describe as the “internal monitor” (Nakamagoe et al. 2000). Models at *both* the neuronal and systems levels are useful – the former to elucidate specific behavior of neural populations and the latter to predict system behavior. It is doubtful that system behavior can ever be predicted by studying small neural populations – the activity of hidden layers in neural networks tells us nothing about how signals are processed. The essence of feedback control system behavior lies *not* in the individual building blocks but in their *interconnections*; from such models we cannot learn about specific neuronal behavior but we can use them to study and predict system behavior and to test specific hypothetical mechanisms for dysfunction.

In order for a model to simulate ocular motor dysfunction (e.g., nystagmus or saccadic intrusions and oscillations) in a truly robust and meaningful manner, it must do more than generate the particular waveform(s) characteristic of that dysfunction. There are an infinite number of ways one can simulate any specific waveform and merely demonstrating that one model, using one method, can do so is insufficient evidence that the model is biologically relevant. What is needed to support a hypothetical model for a specific dysfunction is its demonstrated function within a robust large-scale model of the ocular motor system that contains many, if not all, of the subsystems that are normally present and that might be adversely affected by the dysfunction introduced. Small, limited-scope models of equally small portions of the ocular motor system fail to meet this critical requirement. Although such “bottom-up” models are instructive and may suggest possible mechanisms or anatomical locations, they must be tested within a working model of the whole system before they can rise to the level of realistic, working hypotheses.

A large-scale “top-down” control system model is needed to demonstrate: a broad range of normal re-

sponses when the dysfunction is not present; responses equivalent to those of human patients with the dysfunction; no secondary activation of subsystems that might respond erroneously to the oscillation produced by the dysfunction; and no unexpected neurophysiological interaction with other subsystems. Because of these last points, one cannot eliminate known subsystems to “simplify” the model nor limit it to those subsystems responsible for the desired responses (e.g., one needs to have an intact, *active* pursuit system when testing the saccadic responses of an ocular motor system with an ongoing oscillation to prove that the slow phases do not erroneously activate smooth pursuit). The assumptions commonly made in normal models simply do not apply in the presence of abnormal, internally generated eye movement (e.g., motion on the retina causing retinal slip does *not* imply target motion and must *not* initiate a response). Thus, a robust model, capable of simulating dysfunction, must be more sophisticated than those limited to duplicating stereotypical responses of normals to a limited range of stimuli, or “waveform generators” that are presented as putative hypothetical mechanisms for complex ocular motor dysfunction.

The benefits of such an ocular motor model capable of duplicating both normal and abnormal ocular motor responses are many. First, such a model serves to codify and quantify one’s thinking about the mechanisms responsible for the complex responses of the ocular motor system to various known stimuli. Second, if a particular hypothetical subsystem malfunction can be tested in the context of the whole ocular motor system and it performs as expected from recordings of humans with that dysfunction without either introducing new, uncharacteristic behavior or loss of previously demonstrated behavior, that hypothesis is more strongly supported. Third, such a complex model will, by its nature, contain many hypothetical mechanisms and interactions between subsystems, which may lend themselves to further testing. Finally, if constructed in a modular, subsystem manner, the model can be easily modified by changing specific subsystems as new neurophysiological information about their mechanisms is uncovered. To ensure that the overall model remains robust, each new change or addition must undergo a thorough “backwards compatibility” testing to verify the retention of all previously demonstrated behavior and the absence of new, unphysiological behavior.

In this paper we present the beginnings of such a robust ocular motor system model. Specifically, it is a dual-mode, control-system model that is capable of producing normal saccades and both foveating and de-foveating fast phases in LMLN. Additionally, the model contains a mechanism by which linear slow phases undergo the transition to decreasing velocity slow phases. We made no attempt to differentiate between the hypothetical causes of LMLN but constructed a model that is consistent with each of them; the model’s constant-velocity input to the neural integrator (equivalent to an imbalance in the bilateral, push-pull integrators) may stem from any of the putative causes. A preliminary

attempt to model LMLN was presented elsewhere (Erchul and Dell'Osso 1997). The current model includes programmable Alexander's law behavior (zero to maximal) and fixation conditions (e.g., either eye fixating under either monocular (LN) or binocular (MLN) viewing conditions and is, therefore, capable of simulating the idiosyncratic characteristics of a broad spectrum of individuals with LMLN (Jacobs and Dell'Osso 1999).

Using a robust ocular motor system model with demonstrated capabilities in the simulation of both normal saccadic behavior and that of patients with several saccadic, central, and peripheral dysfunction, we will test the above hypothetical mechanism for LMLN. The ongoing LN or MLN oscillation should not interfere with the normal saccadic system's ability to make accurate and timely saccadic responses to target steps (these will include short-latency corrective saccades where required). The changes in slow-phase velocity induced by the Alexander's law variation with gaze angle should not interfere with the saccadic responses. Waveform transitions resulting from the above slow-phase velocity changes should not interfere with saccadic responses. Direction reversals in LN induced by alternate cover or spontaneous reversals in MLN should not interfere with accurate fixation of a stationary target. Finally, simultaneous Alexander's law variation with gaze angle, waveform transitions, and direction reversals with gaze angle ("adducting-eye fixation") should not interfere with normal saccadic responses.

## 2 Methods

### 2.1 Recording and protocol

The data from 97 LMLN patients of both sexes, ranging in age from infants to the elderly, and including six with Down syndrome (Averbuch-Heller et al. 1999) were used as foundations for our model. The data were recorded in our laboratory over a period of 30 years by either of two methods. Some horizontal eye movement recordings were made using infrared reflection and the remaining data were recorded by means of a phase-detecting revolving magnetic field. Details of the respective equipment, methods, and protocols used may be found in the cited papers. Written consent was obtained from subjects before the testing.

### 2.2 Analysis

Data analysis (and filtering, if required), statistical computation of means and standard deviations, and graphical presentation were performed using custom software written in MATLAB (MathWorks, Natick, Mass.).

### 2.3 Computer simulation

The computer simulation of the control-system model was accomplished using the Simulink component of MATLAB. As the block diagram of Fig. 1 shows, the

## LMLN Block Diagram

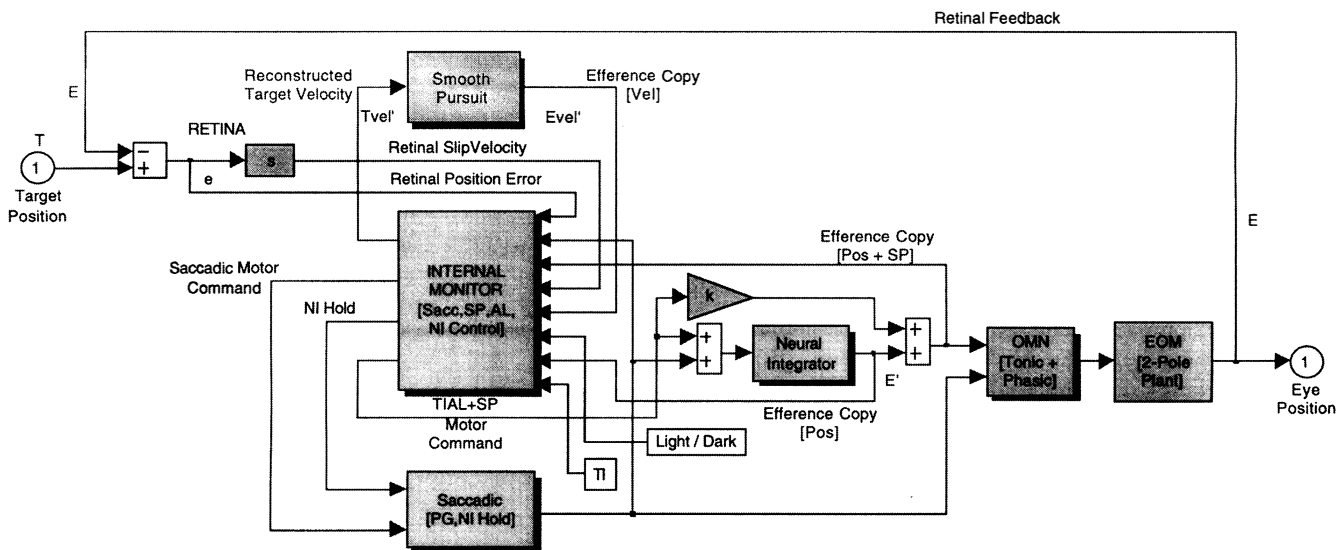


**Fig. 1.** A functional block diagram of the latent/manifest latent nystagmus model showing the basic organization of subsystems and major components. In this and the following figures: *T*, target; *E*, eye; *e*, retinal error; *Tvel'*, reconstructed (perceived) target velocity; *Evel'*, eye-velocity motor command; *E'*, eye-position motor command; *OMN*, ocular motor neuron; *EOM*, extraocular muscle (plant); *TI*, tonic imbalance; *TIAL + SP*, tonic imbalance adjusted by Alexander's law plus smooth pursuit motor command; *NI Hold*, neural integrator

hold signal; *PG*, pulse generator; *Sacc*, *SP*, *AL*, *NI Control*, saccadic, smooth pursuit, Alexander's law, and neural integrator control functional blocks, respectively, in the internal monitor; and other symbols within *square brackets* are signals used by other blocks. Transfer functions of various blocks are shown in their Laplace notation within the block. *Drop shadows* on a functional block indicate that other functional blocks are contained within

## LMLN Model

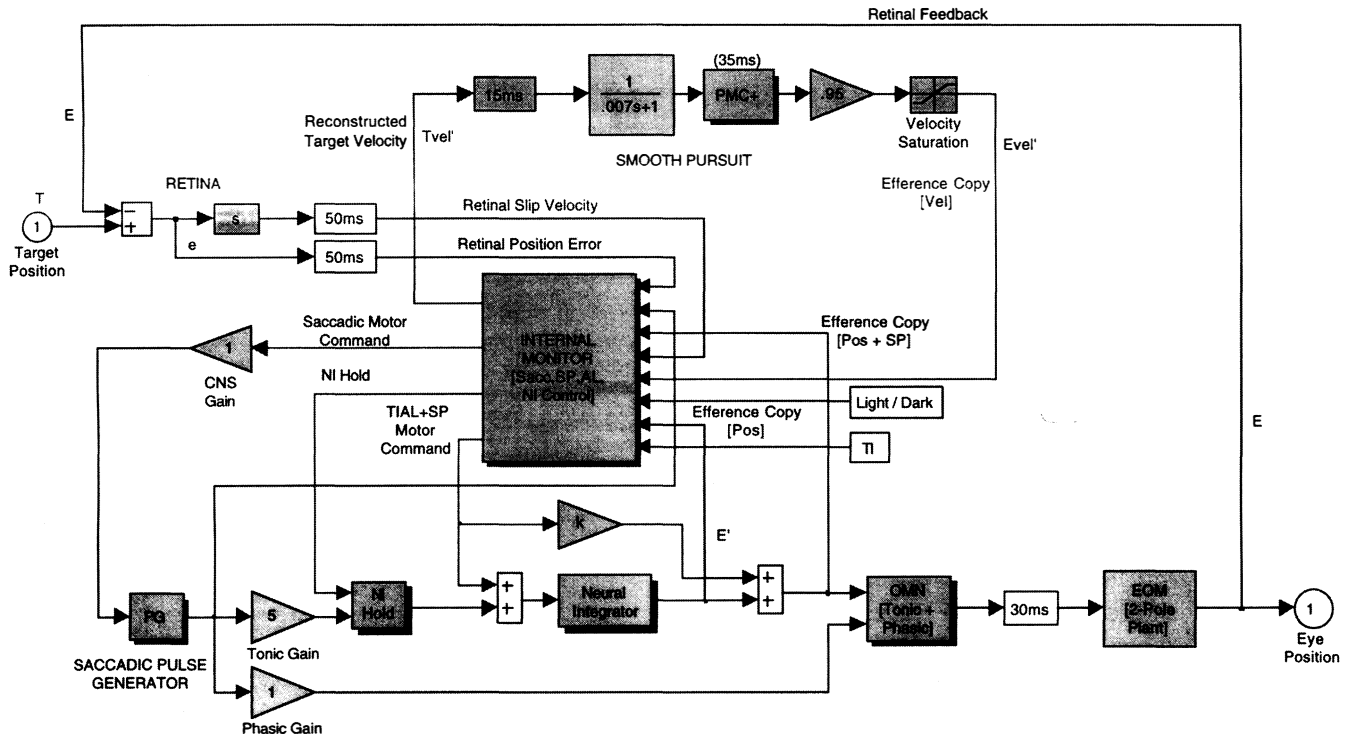


**Fig. 2.** An expansion of Fig. 1 showing the specific components of both the smooth pursuit and saccadic subsystems and also the distributed delays throughout the model. The smooth pursuit system contains distributed delays and gains, a velocity saturation, and a

model is of modular design, consisting of functional building blocks thought to be required for accurate ocular motor control. This allows for easy substitution of any block by an equivalent block, based on new data or personal preference. The modular design facilitates expansion of the model to include additional subsystems and preserves the separation of functions required to produce the wide variety of ocular motor responses exhibited by humans, both normals and those with specific dysfunction. In addition to modularity, the model contains distributed delays (see Fig. 2) that duplicate those known to exist from neurophysiological studies. Figure 2 also shows details of both the smooth pursuit subsystem we used and the pulse generator to neural integrator connections. The model output is that of the fixating eye (either right or left) or of both eyes if conjugacy is assumed. The components of the model (see Figs. 1 and 2) are described below.

*The plant.* Because this is a model of the complex control of several subsystems, a two-pole transfer function was used for the eye plant. It provides an adequate saccadic trajectory, being far better than a single-pole plant and almost as accurate as a plant with one zero and two poles. It has become apparent that a truly realistic simulation of the plant should contain a proprioceptive feedback loop and some form of gain control. Until such a model is derived, the two-pole plant is adequate for our purposes. For simulations

premotor command feedback circuit (*PMC+*) that is responsible for the oscillatory nature of smooth pursuit. The saccadic pulse generator circuitry feeds to the neural integrator through a hold circuit (*NI Hold*) that limits the portion of the pulse that is integrated

requiring the outputs of an additional eye, such as the covered, normal eye in myasthenia gravis, a second plant, driven by the ocular motor neurons, was added.

*The ocular motor neurons.* The summation of tonic and phasic signals at the ocular motor neurons was simulated by a summation with logic to ensure that the output was that of the pulse when a pulse was present. This was done because the very high frequencies exhibited by the burst cells probably serve as an upper limit on the frequency of the motor neurons.

*The common neural integrator.* The common neural integrator consists of a leaky integrator (with a time constant equal to the normal dark-drift time constant of 25 s) around which is a positive feedback gain to offset that leak and produce a non-leaky integrator. Provision was also made to include two such elements to simulate gaze-evoked nystagmus caused by a leak in a subpopulation of the neural integrator cells (Abel et al. 1978).

*The pulse generator.* The pulse generator produces a pulse whose height is determined by a saturating non-linearity and whose duration is determined by a resettable neural integrator and another non-linearity (Abel et al. 1978). A saccadic motor command is passed via a sample-and-hold block to both non-linearities. The pulse-height signal is maintained until the pulse-width signal terminates it. The trailing edge of the pulse

## LMLN Model

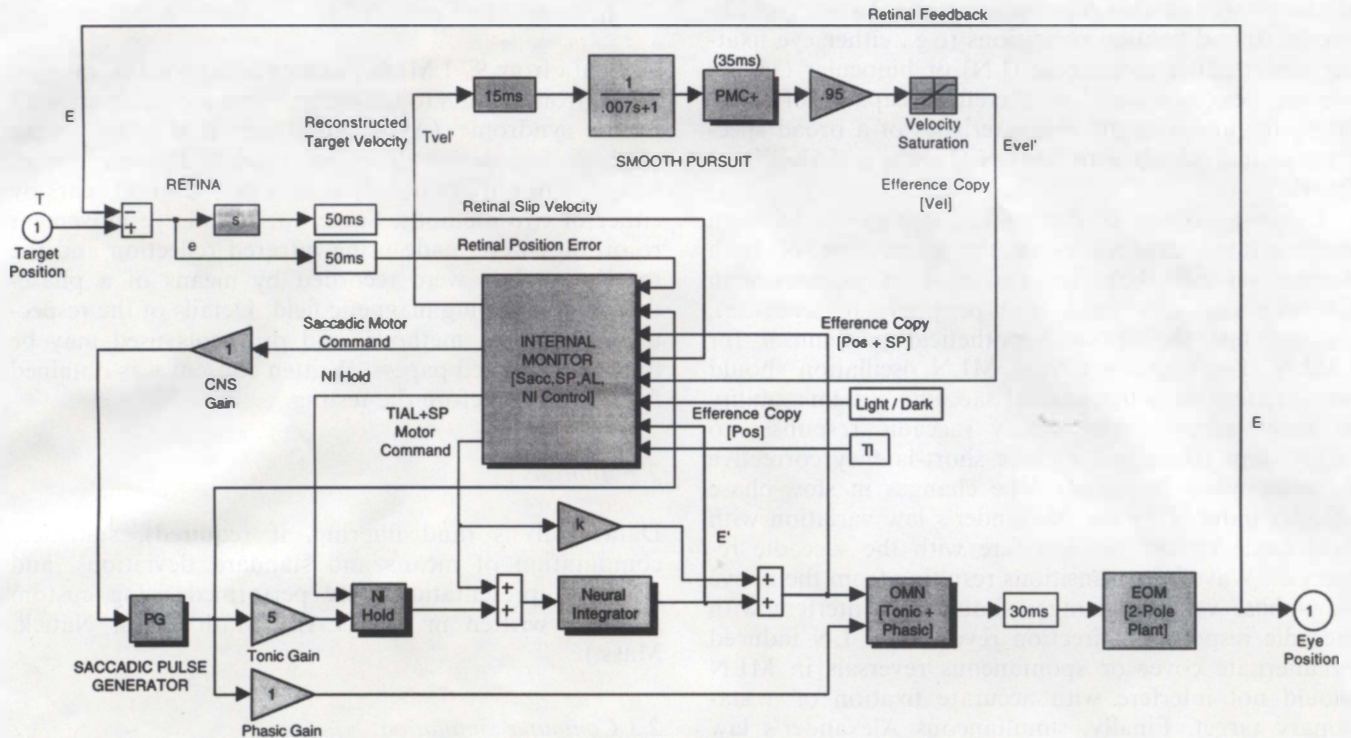


Fig. 2. An expansion of Fig. 1 showing the specific components of both the smooth pursuit and saccadic subsystems and also the distributed delays throughout the model. The smooth pursuit system contains distributed delays and gains, a velocity saturation, and a

model is of modular design, consisting of functional building blocks thought to be required for accurate ocular motor control. This allows for easy substitution of any block by an equivalent block, based on new data or personal preference. The modular design facilitates expansion of the model to include additional subsystems and preserves the separation of functions required to produce the wide variety of ocular motor responses exhibited by humans, both normals and those with specific dysfunction. In addition to modularity, the model contains distributed delays (see Fig. 2) that duplicate those known to exist from neurophysiological studies. Figure 2 also shows details of both the smooth pursuit subsystem we used and the pulse generator to neural integrator connections. The model output is that of the fixating eye (either right or left) or of both eyes if conjugacy is assumed. The components of the model (see Figs. 1 and 2) are described below.

**The plant.** Because this is a model of the complex control of several subsystems, a two-pole transfer function was used for the eye plant. It provides an adequate saccadic trajectory, being far better than a single-pole plant and almost as accurate as a plant with one zero and two poles. It has become apparent that a truly realistic simulation of the plant should contain a proprioceptive feedback loop and some form of gain control. Until such a model is derived, the two-pole plant is adequate for our purposes. For simulations

premotor command feedback circuit (*PMc+*) that is responsible for the oscillatory nature of smooth pursuit. The saccadic pulse generator circuitry feeds to the neural integrator through a hold circuit (*NI Hold*) that limits the portion of the pulse that is integrated

requiring the outputs of an additional eye, such as the covered, normal eye in myasthenia gravis, a second plant, driven by the ocular motor neurons, was added.

**The ocular motor neurons.** The summation of tonic and phasic signals at the ocular motor neurons was simulated by a summation with logic to ensure that the output was that of the pulse when a pulse was present. This was done because the very high frequencies exhibited by the burst cells probably serve as an upper limit on the frequency of the motor neurons.

**The common neural integrator.** The common neural integrator consists of a leaky integrator (with a time constant equal to the normal dark-drift time constant of 25 s) around which is a positive feedback gain to offset that leak and produce a non-leaky integrator. Provision was also made to include two such elements to simulate gaze-evoked nystagmus caused by a leak in a subpopulation of the neural integrator cells (Abel et al. 1978).

**The pulse generator.** The pulse generator produces a pulse whose height is determined by a saturating non-linearity and whose duration is determined by a resettable neural integrator and another non-linearity (Abel et al. 1978). A saccadic motor command is passed via a sample-and-hold block to both non-linearities. The pulse-height signal is maintained until the pulse-width signal terminates it. The trailing edge of the pulse

generator signal is used to initiate a user-definable refractory period after which another saccade can be generated. The non-linear functions were tuned to yield acceptable saccadic trajectories from the two-pole plant and to make hypometric saccades for target steps greater than 17°.

*The saccadic subsystem.* The saccadic system, which includes the pulse generator, responds to abrupt changes in target position and is capable of making short-latency (130 ms) corrective saccades, based on efference copies of eye position motor commands. Such corrective saccades are part of the normal responses to large target changes and to abnormal hypometria or hypermetria. The saccadic system must respond properly to step changes in target position despite the presence of LMLN, ignoring eye position changes due to either the slow or fast phases.

*The smooth pursuit subsystem.* The smooth pursuit system is a modified version of that proposed by Robinson et al. (1986). It was chosen for its transient oscillatory characteristics that we required for our modeling of CN (Dell'Osso and Jacobs 1998). The open-loop gain was set to 0.95 to simulate normal smooth pursuit. It responds to the perceived motion of the target, generating an equivalent velocity signal. The forward path contains a low-pass filter, gain, velocity saturation, and a premotor circuit (PMC+ in Fig. 2). The PMC+ circuit contains an acceleration saturation and an integrator in a negative feedback loop; it controls the oscillatory behavior of the pursuit subsystem. During the saccadic simulations of both normals and those with abnormalities, such as LMLN, it must *not* respond inappropriately to internally generated slow phases during either fixation or in response to target steps.

*The internal monitor.* The internal monitor is a block that subsumes all the computation required for the reconstruction of eye and target position and velocity, and for the programming of saccades and pursuit. Such a grouping is not made on an anatomical basis, but purely on a functional basis; it is *essential* for this model, as the functions it performs have been required by *all* of our past models of ocular motor dysfunction (Dell'Osso 1968; Weber and Daroff 1972; Dell'Osso et al. 1975; Abel et al. 1978, 1980; Doslak et al. 1979, 1982; Dell'Osso and Daroff 1981). Because a moving *oculocentric* coordinate system (the retina) must be used to infer the position and velocity of objects in a head-fixed, real-world coordinate system (*craniocentric*), the internal monitor of afferent and efferent information (or its equivalent) is necessary for all robust models of ocular motor control, normal and abnormal. It makes use of afferent signals from the retina and efferent signals from the brainstem (each with its own distributed delay) to enable the model to detect target changes, to accurately reconstruct target position and velocity, and to differentiate them from eye position and velocity in the presence of motor instabilities. It calculates saccadic

motor commands for voluntary and corrective saccades and for fast phases, perceived target position and velocity, and a signal to control the percentage of every saccadic pulse that should be integrated. Provision is also made for Alexander's law variation of nystagmus slow phases (Doslak et al. 1979, 1982). Without such abilities, we contend that the human ocular motor system could not function (as we know it does function) in the presence of either nystagmus or saccadic instabilities. Additional inputs to the internal monitor are: a light/dark signal, for future simulations of eye movements in the dark; and tonic imbalance (TI) that may be a result of any of a number of mechanisms hypothesized to cause LMLN. As shown in Fig. 3, the internal monitor consists of the following individual functional blocks: target change detection, target position reconstruction (consisting of a model ocular motor neuron and plant plus saccade logic), target velocity reconstruction (consisting of model velocity circuitry and a one-zero, two-pole plant), saccade enable and timing, saccade and drift blanking, neural integrator control, Alexander's law, and braking saccade logic. Figure 4 shows the functional blocks within the saccade enable and timing block. Each functional block makes use of a combination of afferent and efferent signals to achieve its goal of providing needed signals to either other internal monitor blocks or to external functional blocks. Working together, these logic and signal reconstruction blocks allow the ocular motor system to properly differentiate target position/velocity from eye position/velocity and make appropriate decisions to generate responsive eye movements. Further details about the operation of the functional blocks that make up the internal monitor may be found in the Appendix.

*Fast-phase generation.* For the generation of a *foveating* fast phase, the output of the neural integrator is compared with a desired eye-position signal and the difference between them is subjected to a position-signal error threshold. If this error exceeds the threshold, a saccade proportional to the error is generated. When the slow-phase velocity exceeds the velocity threshold (4°/s), a *defoveating* fast phase is generated instead. The transition from foveating to defoveating saccades in the model is based on phase-plane data from LMLN subjects (Dell'Osso et al. 1995). The phase planes showed a significant difference in the presaccadic velocities for the foveating and defoveating cases. However, some showed a region of overlapping slow-phase velocities where either foveating or defoveating fast phases can occur. This could be simulated in the model by a change in the position-error threshold.

*Decreasing velocity slow phases.* Previous studies also showed correlation of fast-phase size with pre- and postsaccadic velocity (Erchul et al. 1996, 1998; Erchul and Dell'Osso 1997). The linear relationship between the size and postsaccadic velocity suggested that an unintegrated pulse (i.e., a saccadic pulse or "stepless" saccade) was being used by the system. The postsaccadic velocities indicated that the pulse was not totally

INTERNAL MONITOR [Sacc,SP,AL,NI Control]

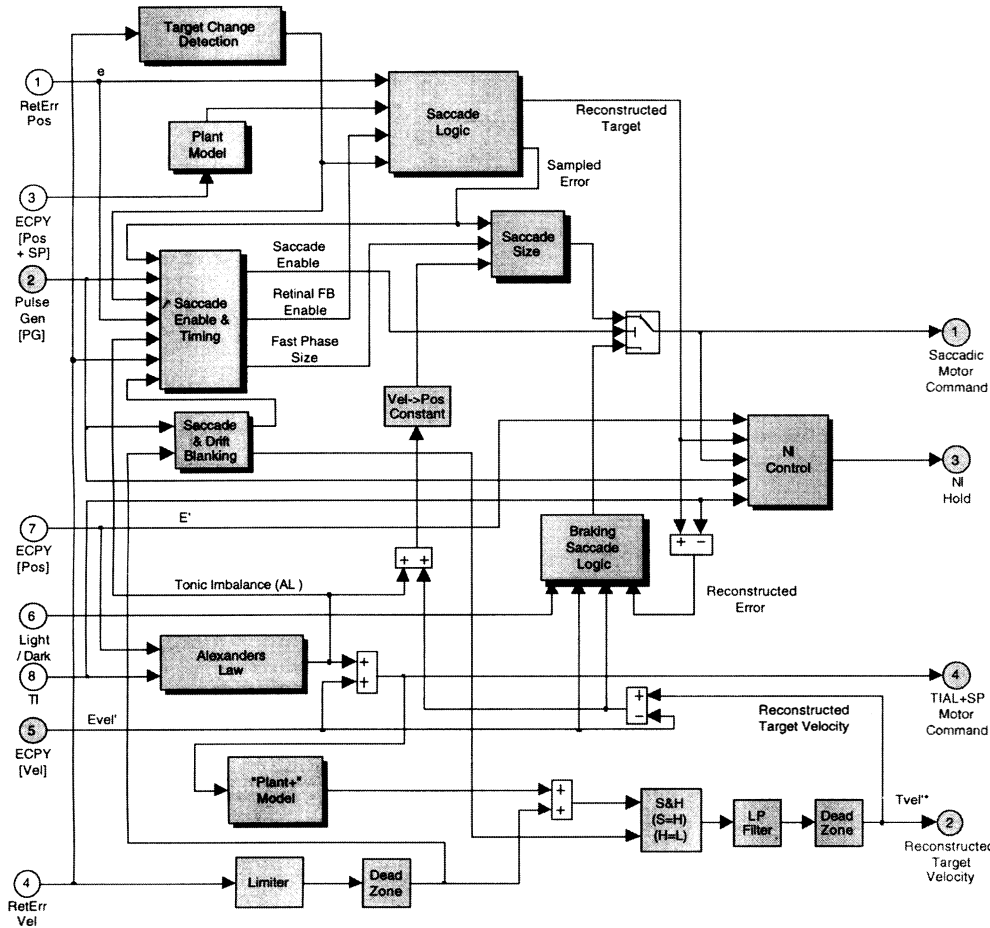


Fig. 3. The arrangement and interconnections of the functional blocks contained within the internal monitor. The major functions of the internal monitor are: detecting target changes, reconstructing target position and velocity, controlling the neural integrator, modifying tonic imbalances (Alexander's law), and determining the timing and amplitudes of saccades and fast phases of nystagmus. The input, output, and other signal labels are consistent with those shown in Figs. 1, 2, and 4. See the Appendix for further definitions

Saccade Enable & Timing

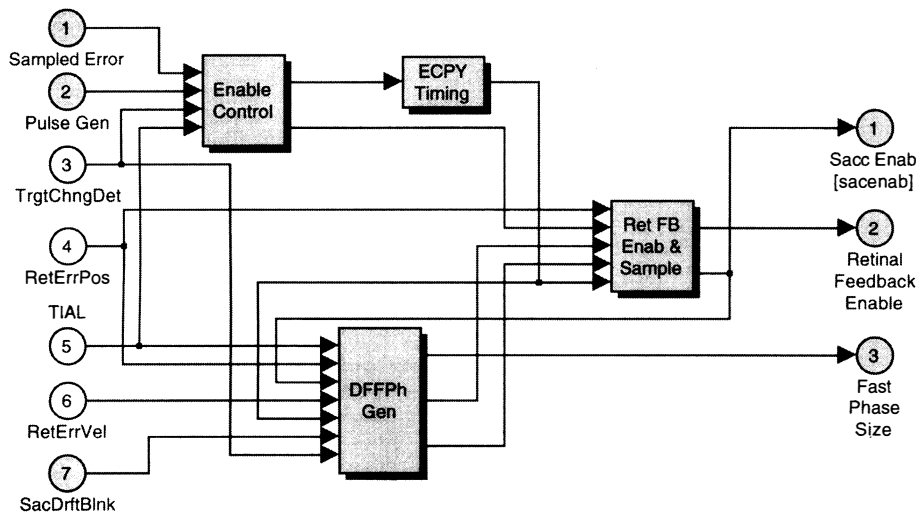
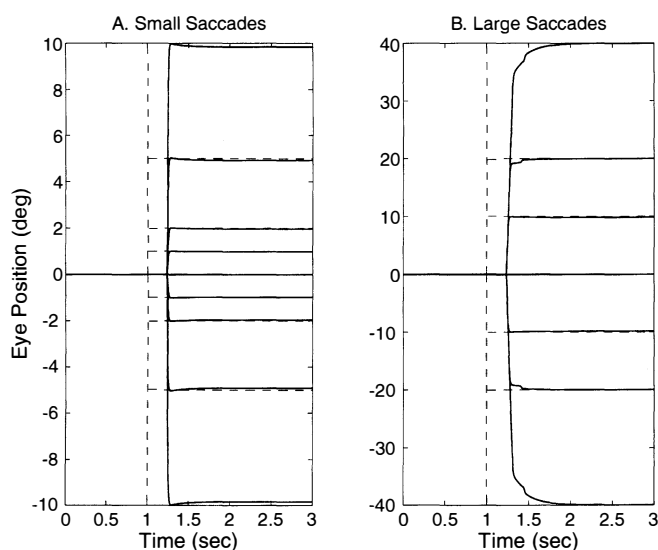


Fig. 4. The arrangement and interconnections of one of the major functional blocks within the internal monitor, saccade enable, and timing blocks. As the drop shadows indicate, each of these functional blocks contains additional functional blocks within. See the Appendix for further definitions

unintegrated and the data suggested that the fast-phase generator produces a pulse of appropriate width and height for a saccade of a relatively small size. Larger saccades are a result of this pulse and a higher, velocity-driven pulse gain. In order to generate the decreasing velocity profiles of LMLN slow phases, additional

mechanisms were required in the model. Increasing the pulse to values that produce saccades greater than that required to foveate the target leads to a larger unintegrated pulse, which is summed with the output from the neural integrator and produces a slow phase with a decreasing velocity.



**Fig. 5A,B.** Model simulations of normal saccadic refixations made by the model from  $\pm 1$ – $40^\circ$  in amplitude. Note that larger refixations are accomplished by primary saccades followed by short-latency corrective saccades, mimicking normal humans. In this and the following figures, target changes and positions are shown *dashed*, and in this and Figs. 7A, 8, 9, and 11, individual model responses to target steps of differing amplitudes (including  $0^\circ$ ) are superimposed

### 3 Results

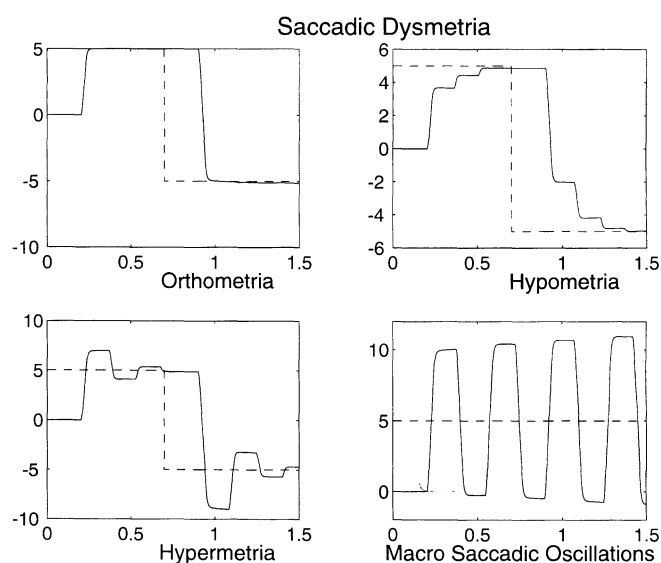
#### 3.1 Normal saccades

Figure 5 illustrates the range over which the model simulates normal saccades. Saccades from  $1^\circ$  to approximately  $17^\circ$  are accurately executed in one movement. Larger saccades show characteristic hypometria followed by a short-interval, non-visually driven (130 ms) corrective saccade. The model correctly responds to target-position changes occurring at any time.

#### 3.2 Abnormal saccades

Dysmetria and oscillations. Simulations of various types of saccadic dysfunction are illustrated in Fig. 6. Hypometria and hypermetria are signs of cerebellar dysfunction and result when the saccadic gain is either too low or high and macrosaccadic oscillations occur when the saccadic gain is  $\geq 2.0$ .

Gaze-evoked nystagmus and myasthenia gravis. The panels in Fig. 7 illustrate the model's simulation of gaze-evoked nystagmus and myasthenia gravis. Gaze-evoked nystagmus (Fig. 7A) was simulated by making the common neural integrator leaky. The two myasthenia gravis examples were simulated by lesioning the plant slightly (Fig. 7B) and including a paresis (Fig. 7C). The movements of the unaffected eye (under cover) were simulated by adding a normal plant to the output of the ocular motor neuron (see Figs. 1, 2). For a more complete demonstration of the simulated variations in gaze-evoked nystagmus, see Abel et al. (1978), and for myasthenia gravis, see Abel et al. (1980).



**Fig. 6.** Model simulations of various types of saccadic dysmetria, including macrosaccadic oscillations, mimicking those recorded in human patients

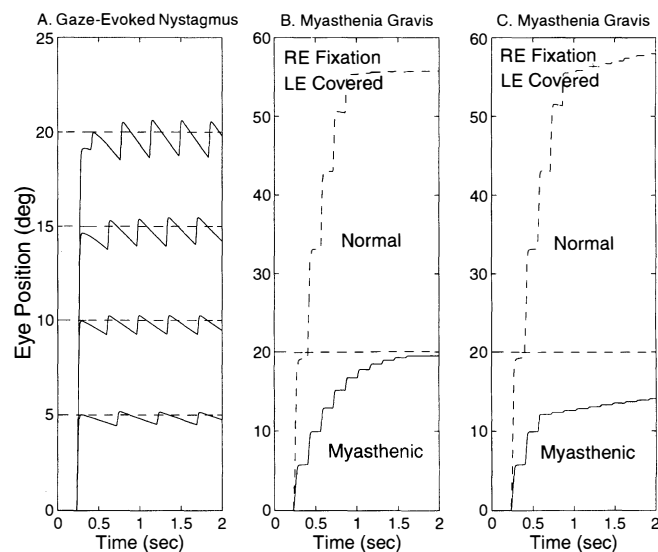


**Fig. 7A–C.** Demonstration of additional types of ocular motor dysfunction that the model is capable of simulating. **A** Simulated gaze-evoked nystagmus produced by lesioning (making leaky) the model's common neural integrator. The nystagmus amplitude increases as gaze is directed from the primary position in either direction; there is no nystagmus in the primary position. **B** Simulated saccades of myasthenia gravis, showing both the hypometric saccadic trajectories of the fixating myasthenic eye and the saccades of the normal, covered eye (shown *dashed*). The ocular plant was lesioned to produce this simulation. **C** Simulated saccades in myasthenia gravis where the myasthenic eye is paretic (i.e., the plant was made to saturate). In **B** and **C**, an additional normal ocular plant was added in parallel to the fixating myasthenic eye to obtain the responses of the normal, covered eye. In this and the following figures: *RE*, right eye; *LE*, left eye

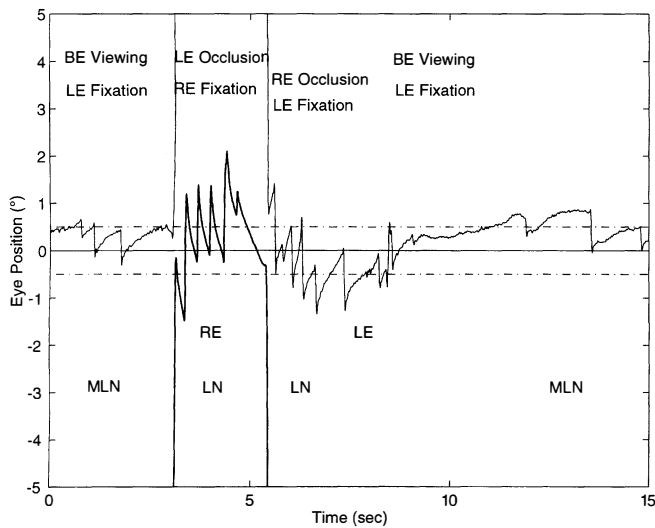


**Fig. 8.** Ocular motor recordings of the fixating eye from a typical subject with esotropia and MLN during binocular viewing and the alternate cover test. Shown are the transitions from binocular viewing (MLN with left-eye fixation in this case), left eye occluded (LN with right-eye fixation), right eye occluded (LN with left-eye fixation), and a return to binocular viewing (MLN with left-eye fixation). During MLN the slow phases were linear with foveating fast phases and during LN the slow phases were decelerating with defoveating fast phases. Some of the fast phases have dynamic overshoots. RE is heavy solid, LE is solid. In this and Fig. 11, dashed lines at  $\pm 0.5^\circ$  indicate the extent of the fovea. In this and the following figures: BE, both eyes

### 3.3 Manifest latent nystagmus

The nystagmus of individuals with MLN (both eyes open) contains linear slow phases and foveating fast phases throughout most gaze angles. Figure 8 shows the movements of the fixating eye during periods of both MLN and LN, the latter being caused by the alternate cover test. This subject preferred to fixate with the left eye while the right eye was in an esotropic position; the resulting MLN was jerk-left. When the left eye was covered, the right eye moved from its esotropic position to take up fixation while the left eye moved to an esophoric position; the resulting LN was jerk-right. When the right eye was covered, the left eye moved from its esophoric position to take up fixation while the right eye moved to an esophoric position; the resulting LN was jerk-left. Finally, when the left eye was uncovered, the LN waveform transitioned to an MLN waveform. The figure demonstrates both the linear slow phases with foveating fast phases of MLN and the decelerating slow phases with defoveating fast phases of LN. Figure 9 shows the model simulation of MLN during saccades and fixation. In Fig. 9A, a small gaze-angle (Alexander's law) effect is simulated and, although slow-phase velocity increases as the fixating right eye abducts, the fast phases remain foveating. In Fig. 9B, a larger gaze-angle effect increases the slow-phase velocity faster as fixation moves in the fixating right eye's abducting direction, and when it exceeds  $4^\circ/s$  the fast phases become larger and defoveating and the slow phases exhibit a decreasing velocity. Note that neither type of MLN interferes with the ability of the saccadic subsystem

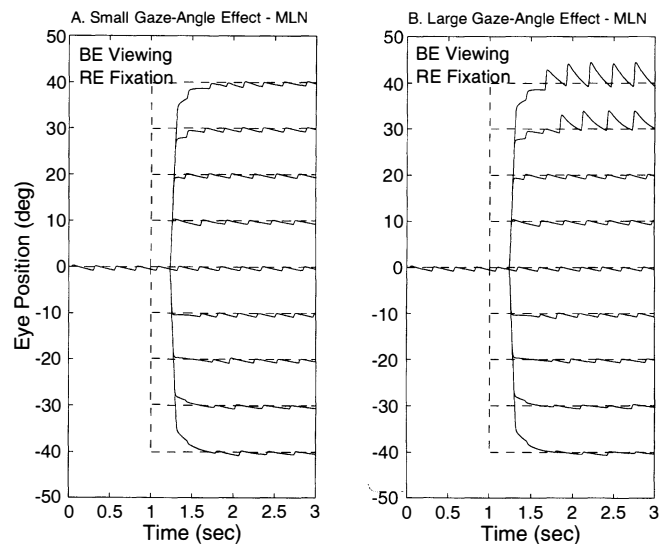


**Fig. 9.** Simulations of the refixations and fixation at various gaze angles of an individual with manifest latent nystagmus and A a small Alexander's law effect or B a large effect. In A, the slow phases remained linear with foveating fast phases, whereas in B, there was a transition to larger, decelerating slow phases and to defoveating fast phases in far abduction of the right, fixating eye

tem to accurately foveate the target, including making corrective saccades when necessary. The amount of Alexander's law effect in a particular simulation is governed by a settable slope parameter.

### 3.4 Latent nystagmus

The nystagmus of individuals with LN (one eye occluded) contains decelerating slow phases and defoveating fast phases throughout most gaze angles (refer to Fig. 8). Figure 10 shows the model simulation of LN during saccades and fixation. In Fig. 10A, a small gaze-angle Alexander's law effect is simulated and, although slow-phase velocity decreases as the fixating right eye adducts, the fast phases remain defoveating except in far adduction. In Fig. 10B, a larger gaze-angle effect decreases slow-phase velocity faster as fixation moves in the fixating right eye's adducting direction, and the slow phases become less than  $4^\circ/s$  at a more central gaze angle, causing smaller, foveating fast phases and linear slow phases. Note again that neither type of LN interferes with the ability of the saccadic subsystem to accurately foveate the target, including making corrective saccades when necessary.

### 3.5 Alternating fixation

The effects of spontaneous alternating fixation on MLN (Fig. 11A) and forced alternating fixation (e.g., as a result of the alternate cover test) on LN (Fig. 11B) is realistically simulated by the model. This was done by simply reversing the sign of the tonic imbalance such that the resulting slow phases were directed toward the

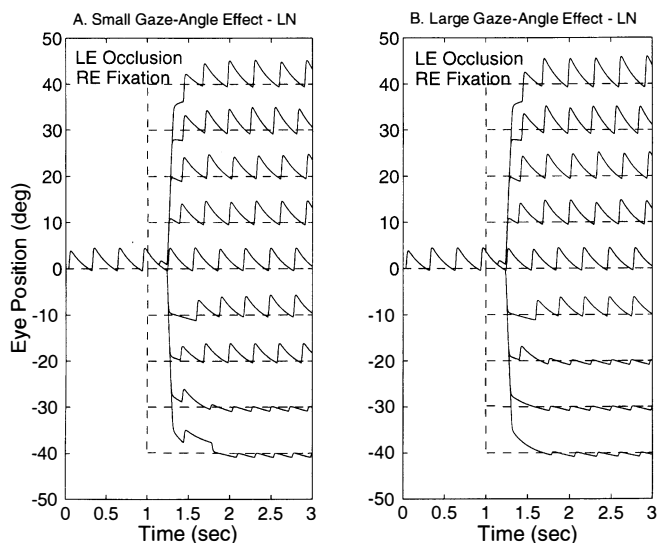


**Fig. 10.** Simulations of the refixations and fixation at various gaze angles of an individual with latent nystagmus and **A** a small Alexander's law effect or **B** a large effect. In **A**, the large, decelerating slow phases and defoveating fast phases did not transition to smaller, linear slow phases and foveating fast phases until far adduction of the fixating right eye, whereas in **B**, the transition occurred closer to primary position

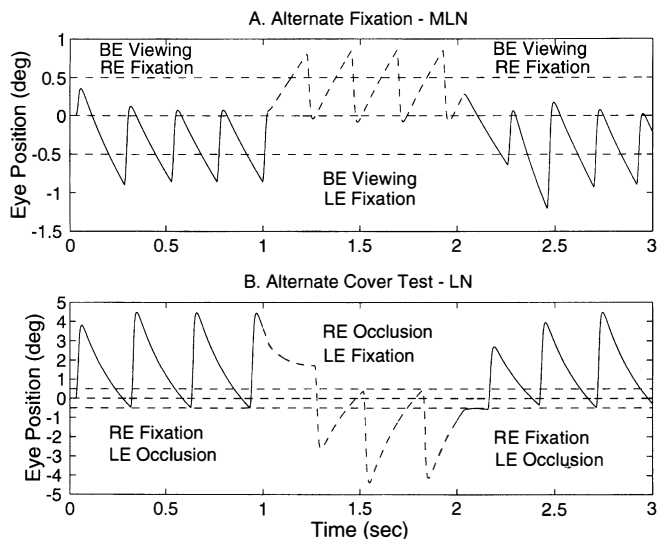


**Fig. 11.** **A** Simulation of the spontaneous alternation in the fixating eye, and the accompanying reversal in nystagmus direction, during fixation seen in individuals with manifest latent nystagmus. In this simulation, the slow phases of the fixating eye (right-left-right) were linear and the fast phases were foveating. **B** Simulation of the responses seen in an individual with latent nystagmus when given the alternate cover test; the nystagmus direction is always that of the fixating eye (right-left-right). In this simulation, the larger slow phases were decelerating and the fast phases were defoveating

non-fixing eye, as would occur in the individual with LMLN under the above two conditions. In Fig. 11A, the MLN slow phases remain linear and the small fast phases remain foveating; in Fig. 11B, larger LN slow phases remain decelerating and fast phases remain defoveating.

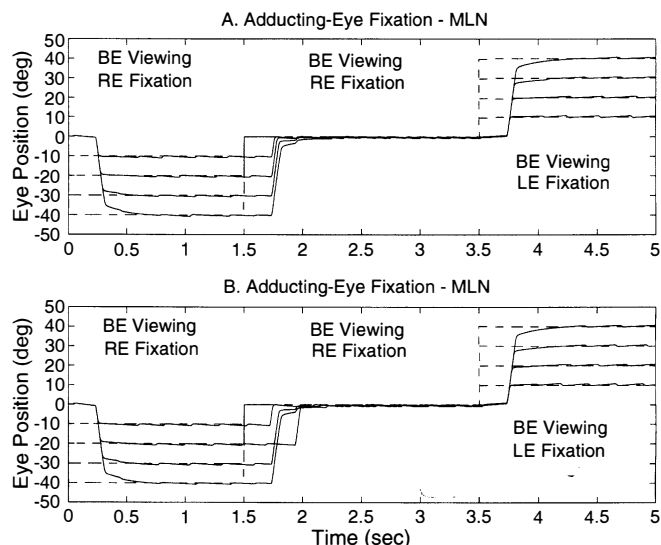


**Fig. 12A,B.** Simulations of the condition of fixation with the adducting eye, commonly seen in individuals with manifest latent nystagmus. In both **A** and **B**, the jerk right nystagmus seen during fixation with the right eye in left gaze diminishes as gaze is directed farther to the left, and the jerk-left nystagmus seen during fixation with the left eye in right gaze diminishes as gaze is directed farther to the right. In **B**, the target change from  $-20^\circ$  to  $0^\circ$  occurred too late to cancel the next right-ward fast phase and the model made the saccade to the primary position after a suitable refractory period

### 3.6 Abducting-eye fixation

As a final demonstration of the model's flexibility and ability to simulate common characteristics of LMLN while simultaneously responding correctly to step changes in target position, the phenomenon of fixation with the adducting eye (i.e., looking over the nose) is demonstrated in Fig. 12. This usually results in a head turn to the opposite direction and often produces confusion with CN and the mistaken impression that CN can have two nulls. In both Fig. 12A and B, the fixating eye has minimal MLN in far adduction (due to Alexander's law) and the direction spontaneously reverses from jerk-right in left gaze to jerk-left in right gaze with the accompanying change in the fixating eye. Again, the MLN does not prevent the saccadic subsystem from foveating the target and, as is illustrated in Fig. 12B, when the target change occurs too late to suppress the next fast phase, the voluntary saccade is correctly made following an intersaccadic refractory interval (saccade from  $-20^\circ$  to  $0^\circ$ ).

## 4 Discussion

We constructed a model of the normal ocular motor control system that includes a hypothetical mechanism for generating LMLN and the transition between foveating and defoveating fast phases. This transition is based on the following observations and assumptions: the stimulus for the oscillation is a tonic imbalance signal that produces a linear slow eye movement directed

opposite to the fixating eye; normally foveating fast phases become defoveating when the speed of the linear slow phases exceed an idiosyncratic threshold value (due to covering one eye or Alexander's law variation (Doslak et al. 1979, 1982)); and the transition from linear to decelerating slow phases is a consequence of common neural integrator control, allowing integration of only that portion of saccadic pulses that make the integrator output signal equivalent to that of the desired eye position (Abel et al. 1978). This is consistent with the observed shape of the slow phases responsible for the generation of LMLN in human subjects. The model also simulates saccadic dysfunctions, gaze-evoked nystagmus, and myasthenia gravis. Although the model contains a smooth pursuit system, we present only the saccadic and fixation responses in this study; *neither the smooth pursuit system nor the braking saccade logic (needed for CN simulations) was improperly activated during any of the simulations.*

#### 4.1 Hypotheses of the model

We hypothesized that an internal monitor could make use of afferent retinal and efferent motor information to detect changes in target position and to accurately differentiate target position and velocity from internally generated eye position and velocity (e.g., resulting from LMLN). We also hypothesized that LMLN is ultimately caused by a tonic imbalance (i.e., constant-velocity signal) to the common neural integrator that causes both eyes to move in a direction opposite to the fixating eye and with greater velocity when one eye was occluded. In addition, we hypothesized that when the slow-phase velocity exceeded  $4^\circ/\text{s}$ , the foveating fast phases of the LMLN would undergo a transition to defoveating fast phases and the resulting slow phases would have an decreasing velocity due to unintegrated portions of the fast-phase pulses. Finally, we hypothesized that, due to Alexander's law, slow-phase velocity increased as gaze was directed in the abducting direction of the fixating eye and that would ultimately cause the transition from foveating to defoveating fast phases.

#### 4.2 Foundations of the model

This model was built on the foundations laid in previous models of ocular motor dysfunction with the aim that the model be *robust* in its range of simulations and its insensitivity to internal errors (i.e., the model produces a wide variety of realistic, goal-directed outputs and recovers from "mistakes"). From those models, we incorporated a pulse generator with a resettable neural integrator, an internal monitor to reconstruct target position and velocity, and a common neural integrator under feedback control to determine what percentage of each pulse requires integration. In addition, we incorporated a tonic imbalance signal whose primary-position amplitude depended on whether both eyes were open or one was occluded, and whose final amplitude

varied with gaze angle to a settable degree. We demonstrated the ability of this model to simulate both normal and abnormal saccadic responses, several types of ocular motor dysfunction, and saccadic and fixation responses of subjects with LMLN under different viewing conditions.

#### 4.3 Evolving the model

Although previous models were limited in the scope of their simulations, all were designed to simulate both normal and abnormal responses and, thereby, yielded insights into normal ocular motor control. In contrast, models that were restricted to normal responses did not reveal the complexities inherent in the accurate control of eye movement. As a result, such models tended to be simplistic (e.g., the final common neural integrator was used for both eye position and to control the pulse width of the saccadic burst neurons), usually contained unjustifiable assumptions (e.g., retinal image motion equals target motion), and were inadequate representations of the wide range of human ocular motor control. The following aspects of human ocular motor control were only recognized when attempts were made to simulate dysfunction: the necessity of employing efference copy of motor commands; the existence of a separate *resettable* neural integrator for pulse generation; and that the common neural integrator does not, and *should not*, integrate all pulses it receives but only those (or part of those) required to match the eye-position motor command to perceived target position. Thus, our simulation makes extensive use of efference copy of motor output signals (the *internal monitor*), as first required in a model of CN (Dell'Osso 1968), later in a study of normal corrective saccades (Weber and Daroff 1972), and in models of square-wave pulses (previously designated as, macro square-wave jerks) (Dell'Osso et al. 1975), gaze-evoked nystagmus (Abel et al. 1978), and myasthenia gravis (Abel et al. 1980). It also contains a resettable neural integrator in the pulse generator (Abel et al. 1978, 1980) that is distinct from the common neural integrator responsible for maintaining eye position, and it utilizes feedback control of the saccadic pulse input to the common neural integrator, as required by the gaze-evoked nystagmus model (Abel et al. 1978).

As we added individual features to the model to broaden its range of simulations, each was followed by an extensive retesting of all previous simulations to ensure that no loss of function occurred. Specific attempts that failed to accomplish their goal or interfered with existing functions were discarded and those that worked were retained and refined. In this manner, we interactively *evolved* the model over a period of several years. Finally, the LMLN model contains internal-monitor features required by our preliminary model of CN (Dell'Osso and Jacobs 1998) that, although not necessary for LMLN simulations, were retained and did not interfere with them. Specifically, the determination of perceived target velocity (used to drive

the smooth pursuit subsystem) was not confounded by the slow phases (linear or decelerating) of LMLN, and neither braking nor foveating saccades were mistakenly generated by the functional block responsible for their insertion into CN waveforms. Thus, in addition to LMLN, this model retains the capability of simulating normal eye movements and, with proper settings (i.e., “lesions”), the other neurological conditions of its predecessors (e.g., gaze-evoked nystagmus and myasthenia gravis). It is our goal to marry the LMLN and CN models into a unitary ocular motor control system model that can be used to simulate many – if not all – of the behaviors exhibited by both normal individuals and those with specific ocular motor dysfunction.

#### 4.4 The dual-mode nature of the model

The automatic transition between foveating and defoveating fast phases in this simulation is affected by the interaction of the dynamics of the eye plant with presaccadic slow-phase velocity and position-error threshold. Although the decelerating slow phases could have significant implications for visual acuity, the method for their generation is not critical for the basic mechanism proposed here as an explanation for foveating and defoveating fast phases in LMLN. The model demonstrates how visual acuity could be improved by the defoveating fast-phase strategy if the final slowing of decelerating LMLN slow phases could be accomplished by a fixation subsystem. A more sophisticated model of LMLN should include a fixation mechanism that uses position- and velocity-signal feedback to further decrease the slow-phase velocity. In addition, the model could include a mechanism for the generation of dynamic overshoots. However, this is not critical for the simulation presented here concerning the transition between foveating and defoveating fast phases.

#### 4.5 Emergent behavior of the model

One of the marks of the biological relevance of a model is its ability to exhibit behavior not designed into it. Examination of some of the responses shown in Fig. 9, 10, and 12 reveal such behavior. In Fig. 9A: the corrective saccades needed to acquire the targets at  $20^\circ$  and  $30^\circ$  were altered by the fast phases of the MLN; the postsaccadic drift after the corrective saccade to  $40^\circ$  was diminished by the oppositely directed slow phase of the MLN; extended slow phases after the initial saccades to  $-10^\circ$  and  $-20^\circ$  acquired the target and suppressed the corrective saccade that would have occurred for  $-20^\circ$ ; and the corrective saccades to  $-30^\circ$  and  $-40^\circ$  were diminished by the MLN slow phases. In Fig. 9B, in addition to similar interactions, the transitions from foveating to defoveating fast phases at  $30^\circ$  and  $40^\circ$  were delayed by the interaction between postsaccadic drift and oppositely directed MLN slow phases. In Fig. 10A: postsaccadic drift delayed the transition to foveating fast phases at  $-30^\circ$  and  $-40^\circ$  (the same thing occurred at  $-20^\circ$  in the plots shown in Fig. 12B). Also, the defoveating

fast phase occurring just after the initial saccade to  $-40^\circ$  delayed but did not prevent, the needed corrective saccade (i.e., the model acted to correct itself). Figure 10B also demonstrates how postsaccadic drift and slow phases combined to supplant the otherwise required corrective saccades needed to acquire the  $-30^\circ$  and  $-40^\circ$  targets. Figure 12 exhibited similar emergent behavior, and in Fig. 12B the initial saccade to  $-20^\circ$  was delayed by the timing of a fast phase that occurred before the normal saccadic latency (again, the model corrected itself). All of these responses, predicted by the model, were due to interactions of different hypothetical mechanisms for both normal and abnormal behavior and, significantly, these behaviors have all been documented in the ocular motility recordings of subjects with LMLN.

#### 4.6 A robust ocular motor system model as a research tool

Because MATLAB/Simulink is widely used and this model is of modular construction, it can serve as a *test bed* for other investigators to test hypothetical mechanisms. The existing simulations of specific subsystems can be replaced by newer ones as they are developed, models of other subsystems can be added as needed (e.g., vestibular or optokinetic), models of other dysfunctions can be tested (e.g., saccadic intrusions and oscillations), and both students and researchers can use it to study the ocular motor system under both normal and abnormal conditions. Toward that end, we plan to make all of the constituent subsystems available as MATLAB files to investigators who request them and, eventually place them on a web site for easy downloading.

#### Appendix: The internal monitor

The major functions of the internal monitor are described in Sect. 2. Below are descriptions of the operating principles of each functional sub-block whose interconnections (shown in Figs. 3, 4) form the internal monitor.

*Target change detection.* There are four implementations of this circuitry. The first uses retinal error velocity to detect all target changes of  $\geq 1^\circ$  at all times. The second also uses the pulse generator (“Pulse Gen”) signal to detect all target changes of  $> 0.1^\circ$  except during a saccade. The third uses the same two signals and a sampled, reconstructed retinal error to detect all target changes  $> 0.1^\circ$ , except during a saccade when it detects all target changes  $> 0.2^\circ$ . The fourth uses the initial two signals and a sampled, reconstructed retinal slip velocity to detect all target changes  $> 0.1^\circ$ , except during a saccade when it detects all target changes  $> 1^\circ$ . At present, we are using the first implementation.

*Plant model and saccadic logic.* Retinal error position is summed with the efference copy of eye position after the latter is passed through a model of the OMN and two-

pole plant; appropriate delays are in place. The resulting signal is reconstructed target position which is sampled when either a target change is detected or a retinal feedback sample is called for by the saccade enable and timing circuitry.

*Target velocity reconstruction.* Retinal error velocity is limited and passed through a dead zone ( $0.1^\circ/\text{s}$ ) and then summed with the efference copy of eye velocity after the latter is summed with tonic imbalance and passed through a model of the one-zero, two-pole (“Plant+”); appropriate delays are in place. The resulting signal is sampled or held, based on the signal from the saccade and drift blanking circuit. This signal is low-pass filtered and passed through a dead zone ( $0.2^\circ/\text{s}$ ) to yield reconstructed target velocity, which is the input motor command signal to the smooth pursuit circuitry.

*Saccade enable and timing.* Using the inputs shown in Fig. 4, these blocks determine when to output commands that enable saccades to be generated, to sample the retina, and to produce a defoveating fast phase of a particular size. The sub-blocks are: enable control, efference copy (“ECPY”) timing, retinal feedback (“Ret FB”) enable and sample, and defoveating fast-phase generation (“DFFPh Gen”). The enable control circuitry sends output signals to both the ECPY timing and Ret FB enable and sample circuits. The output from the latter directly enables a saccade to be initiated. Its second output is retinal FB enable, which allows sampling of a new reconstructed target signal; target change detection also allows such sampling. The third output (from defoveating fast-phase generation) is fast-phase size, that is added to a sampled, reconstructed retinal error signal to determine saccade size via the saccadic motor command, which is sent to the pulse generator.

*Enable control.* This uses sampled, reconstructed retinal error (after a  $0.3^\circ$  dead zone), pulse gen, target change detection, and tonic imbalance acted on by Alexander’s law (“TIAL”) to determine if an ECPY (i.e., “corrective”) saccade or a Ret FB (i.e., “fixation”) saccade should be enabled. If the sampled error is non-zero and it has been less than 150 ms since the last detected change in target position, Pulse Gen is passed to the output, “ECPY Timing”. If, on the other hand, 150 ms has elapsed since the last detected target change, the “Ret FB Enab” output will be high; that output passes to the Ret FB enable and sample circuitry.

*ECPY timing.* This acts on the input signal from enable control. It outputs a signal to the Ret FB enable and sample circuitry that is 10 ms long and starts 130 ms after Pulse Gen concludes.

*Ret FB enable and sample.* This uses five inputs: retinal error position, a signal from the enable control circuitry, two signals from the DFFPh Gen circuitry, and one from the ECPY timing circuitry. Its outputs are signals that enable either retinal feedback or saccades. The first signal allows sampling of reconstructed target position.

Each input from ECPY timing resets the circuitry until a latency of 330 ms expires and sets the output high. The “Ret FB Enable” signal produces “Sacc Enab” (see above). Before a “Ret FB Enab” signal is created, one of five criteria must be satisfied, several of which depend on specific combinations of the five inputs to the Ret FB enable and sample circuitry. Two criteria that directly trigger a “Ret FB Enable” output are a “Ret FB Enab & Spl” signal from the enable control circuitry and a signal from within this block. Each of two other criteria results from the outputs of multi-input AND gates. The first AND gate requires that four conditions be met: 200 ms has elapsed since the last saccade enabling signal, the tonic imbalance signal must be zero, the retinal error signal must have a magnitude  $>0.5^\circ$ , and the retinal error velocity signal must be high. The second AND gate also requires that four conditions be met: 200 ms have elapsed since the last saccade enabling signal, retinal error has to be non-zero, retinal error velocity must be high, and tonic imbalance must be non-zero. The final criterion that triggers “Ret FB Enab” is the output of an AND gate when the magnitude of the retinal error is higher than a  $0.5^\circ$  threshold. This triggers a “corrective” saccade.

*Defoveating fast-phase generation.* This uses seven inputs: “TIAL”, “Ret Err Pos”, “Ret FB Enable” from the Ret FB enable and sample circuitry, “Ret Err Vel”, “ECPY Enable” from the ECPY Enable circuitry, “Sac Drft Blnk”, and “Trgt Chng Det”. Its major output is “Fast Phase Size”, which is “TIAL” multiplied by  $-0.8$  after passing through a dead zone of  $4^\circ/\text{s}$ . It is an output if either “Ret FB Enable” or “ECPY Timing” signals are high and at least 200 ms has elapsed since the last “Trgt Chng Det” signal; if both are low, “Fast Phase Size” is zero. Two other outputs are signals related to “Ret Err Vel” and “TIAL” that are used by Ret FB enab and sample.

*Saccade size.* This uses “Fast Phase Size”, “Sampled Error” (retinal), and a modified velocity signal to calculate the magnitude of the saccade to be generated by the pulse generator.

*Saccade and drift blanking.* The saccade and drift blanking circuitry prevents other logic from evaluating steady-state target, eye, or retinal variables during, or immediately after saccades. It creates a blanking signal that lasts for the length of the saccadic pulse plus 70 ms, using a delayed “Pulse Gen” signal. The output signal is also used to prevent the effects of postsaccadic drift from adversely affecting calculation of reconstructed target velocity.

*Neural integrator control.* When a TI is present, the NI control circuitry allows the NI to integrate the output of the pulse generator until its output (desired eye position) is equal to the reconstructed target position. When NI control is active, the “Pulse Gen” signal is not integrated by the NI. “NI Hold” is set to zero when both “Pulse Gen” and the reconstructed error signal are non-zero.

During “Pulse Gen”, “NI Hold” remains low until a reconstructed retinal error signal crosses zero, whereupon “NI Hold” is set high. It is also set high if “Pulse Gen” terminates. In the absence of a tonic imbalance (TI = 0), the NI integrates all “Pulse Gen” signals. Other conditions (e.g., for gaze-evoked nystagmus or smooth pursuit) need to be added to activate this circuitry to allow the NI to hold its value when it has arrived at the correct eye position.

*Alexander's law.* This mechanism uses efference copy of eye position to modulate the TI input and produce “TIAL”. The eye-position signal is multiplied by the Alexander's law slope and filtered before summing with TI. Depending on the sign of TI, this sum is kept greater than or less than zero, and is passed on to a final switch that only produces an output if TI is present. Differing amounts of the Alexander's law effect are simulated by the value of the Alexander's law slope.

*Braking saccade logic.* This circuitry uses sampled “Reconstructed Error” (retinal position), sampled, reconstructed retinal slip velocity, and desired eye velocity to determine if the conditions for generating a braking saccade are met. Braking saccades occur in many CN waveforms and always occur in the direction opposite to eye motion if the eye is moving away from the target. First, “Reconstructed Error” is used by the braking saccade logic circuit to determine if retinal error is increasing (calling for a braking saccade) or decreasing (no braking saccade). If this criterion for a braking saccade is met, its magnitude is determined within limits. Second, an estimate of retinal slip velocity is compared to a threshold; if it exceeds it, the second criterion for a braking saccade is met. Third, the direction of desired eye velocity is determined and used to assign the direction of the braking saccade. If the desired eye acceleration falls below threshold, a braking saccade is enabled for a period of time determined by a timing circuit.

*Acknowledgements.* The authors wish to acknowledge the contributions of D.M. Erchul to preliminary simulations that helped lead to the present model. This work was supported in part by the Office of Research and Development, Medical Research Service, Department of Veterans Affairs.

## References

- Abel LA, Dell'Osso LF, Daroff RB (1978) Analog model for gaze-evoked nystagmus. *IEEE Trans Biomed Eng* 25: 71–75
- Abel LA, Dell'Osso LF, Schmidt D, Daroff RB (1980) Myasthenia gravis: analogue computer model. *Exp Neurol* 68: 378–389
- Averbuch-Heller L, Dell'Osso LF, Jacobs JB, Remler BF (1999) Latent and congenital nystagmus in Down syndrome. *J Neuroophthalmol* 19: 166–172
- Dell'Osso LF (1968) A dual-mode model for the normal eye tracking system and the system with nystagmus. PhD thesis, University of Wyoming, Laramie, Wyo., pp 1–131
- Dell'Osso LF (1985) Congenital, latent and manifest latent nystagmus – similarities, differences and relation to strabismus. *Jpn J Ophthalmol* 29: 351–368
- Dell'Osso LF (1994) Congenital and latent/manifest latent nystagmus: diagnosis, treatment, foveation, oscillopsia, and acuity. *Jpn J Ophthalmol* 38: 329–336
- Dell'Osso LF, Daroff RB (1981) Clinical disorders of ocular movement. In: Zuber BL (ed) *Models of oculomotor behavior and control*. CRC, Boca Raton, Fla., pp 233–256
- Dell'Osso LF, Jacobs JB (1998) An preliminary model of congenital nystagmus (CN) incorporating braking saccades. *Invest Ophthalmol Vis Sci* 39: S149
- Dell'Osso LF, Troost BT, Daroff RB (1975) Macro square wave jerks. *Neurology* 25: 975–979
- Dell'Osso LF, Schmidt D, Daroff RB (1979) Latent, manifest latent and congenital nystagmus. *Arch Ophthalmol* 97: 1877–1885
- Dell'Osso LF, Traccis S, Abel LA (1983a) Strabismus – a necessary condition for latent and manifest latent nystagmus. *Neuroophthalmology* 3: 247–257
- Dell'Osso LF, Ellenberger JC, Abel LA, Flynn JT (1983b) The nystagmus blockage syndrome: congenital nystagmus, manifest latent nystagmus or both? *Invest Ophthalmol Vis Sci* 24: 1580–1587
- Dell'Osso LF, Leigh RJ, Sheth NV, Daroff RB (1995) Two types of foveation strategy in ‘latent’ nystagmus. Fixation, visual acuity and stability. *Neuroophthalmol* 15: 167–186
- Doslak MJ, Dell'Osso LF, Daroff RB (1979) A model of Alexander's law of vestibular nystagmus. *Biol Cybern* 34: 181–186
- Doslak MJ, Dell'Osso LF, Daroff RB (1982) Alexander's law: a model and resulting study. *Ann Otol Rhinol Laryngol* 91: 316–322
- Erchul DM, Dell'Osso LF (1997) Latent nystagmus fast-phase generation. *Invest Ophthalmol Vis Sci* 38: S650
- Erchul DM, Jacobs JB, Dell'Osso LF (1996) Latent nystagmus fast-phase generation. *Invest Ophthalmol Vis Sci* 37: S277
- Erchul DM, Dell'Osso LF, Jacobs JB (1998) Characteristics of foveating and defoveating fast phases in latent nystagmus. *Invest Ophthalmol Vis Sci* 39: 1751–1759
- Ishikawa S (1979) Latent nystagmus and its etiology. In: Reinecke RD (ed) *Proceedings of the Third Meeting of the International Strabismological Association*. Grune and Stratton, New York, pp 203–214
- Jacobs JB, Dell'Osso LF (1999) A dual-mode model of latent nystagmus. *Invest Ophthalmol Vis Sci* 40: S962
- Kommerell G, Mehdorn E (1982) Is an optokinetic defect the cause of congenital and latent nystagmus? In: Lennerstrand G, Zee DS, Keller EL (eds) *Functional basis of ocular motility disorders*. Pergamon, Oxford, pp 159–167
- Nakamagoe K, Iwamoto Y, Yoshida K (2000) Evidence for brainstem structures participating in oculomotor integration. *Science* 288: 857–859
- Robinson DA (1994) Implications of neural networks for how we think about brain function. In: Cordo P, Harnad S (eds) *Movement control*. Cambridge University Press, Cambridge, pp 42–53
- Robinson DA, Gordon JL, Gordon SE (1986) A model of smooth pursuit eye movements. *Biol Cybern* 55: 43–57
- Weber RB, Daroff RB (1972) Corrective movements following refixation saccades: type and control system analysis. *Vision Res* 12: 467–475